Estimating the Geometry and Mass of an Ore Body Using a Gravity Survey.

Richard Williams

ABSTRACT

The lateral extent of an ore body at a depth of approximately 1000 m was estimated using the results of a gravity survey. The Bouguer anomaly was determined by applying normal, drift, elevation and terrain corrections to the raw gravity data. The extent of the anomaly was further investigated using the first horizontal derivative of the gravity anomaly. After corrections, a negative density anomaly with a mininum value of $-3.6836\,\mu$Gal was isolated. The results suggested the presence of an irregularily shaped ore body with rough dimensions of 20 km by 15 km and density lower than that of the surrounding rock. The total mass of the anomalous body was estimated to be 5.3×10^9kg.

THEORY

A subsurface density anomaly produces an anomalous gravity effect that can be measured at the surface. A gravitational survey can be performed over a region to locate subsurface density anomalies, but variations in the measured gravity due to lattitude, elevation, terrain, tidal effects and instrument drift can be of the same mangitude or greater than those produced by the anomalous density. Corrections for these variations must be made in order to reveal the gravitational signature of the anomalous body (Long and Kaufmann, 2013).

The value of theoretical gravity g_t varies with lattitude θ due to the rotation of the Earth as well as its non-spherical shape (Long and Kaufmann, 2013). Survey data is corrected for theoretical gravity by subtracting it from the measured gravity. Latitude corrections are based on the International Gravity Formula (IGF). The IGF calculates the theoretical gravity based on an ellipsoidal earth shape. Moritz (2000) gives an equation based on an updated reference ellipsoid

$$g_t(\theta) = 9.780327\left(1 + 0.0053024\sin^2(\theta) - 0.0000058\sin^2(2\theta)\right) \tag{1}$$

The readings from a gravimeter placed in one position will vary over time. This variation is due to tidal effects and instrument drift (Burger et al., 2006). Tidal variation is caused by a change in the relative position of the moon and the sun over the course of the survey. The tidal effect Δg_{tide} can be determined by measuring the change in absolute gravity over time using an absolute gravimeter at a base station. Instrument drift is a small, long-period fluctuation in the readings of the gravimeter. It can be corrected by performing the survey in smaller closed loops that return to the same point one or more times. If the period of these survey loops is small compared to the period of instrument drift, corrections can be made to the survey data by assuming the drift over the loop is linear. Karwchewski (2016) provides a formula to apply corrections over each loop using a linear interpolation

$$\Delta g_{\text{drift}}(t) = \frac{g_2 - g_1}{t_2 - t_2}(t - t_1) \tag{2}$$

where g_2 and t_2 are the gravity and time measurements at the end of the loop, g_1 and t_1 are the measurements at the begining of the loop, and t is the time of the measurement being corrected.

The gravitational acceleration decreases with increasing elevation due to increased distance from the Earth's centre of mass. The free-air correction Δg_{FA} accounts for this change in gravity. The gravitational acceleration g due to the earth is

$$g = \frac{GM_e}{R_e^2} \tag{3}$$

where M_e is Earth's mass and R_e is the distance from its centre of mass. The vertical gradient can be determined by taking the first derivative of equation 3

$$\Delta g_{FA} = \frac{dg}{dR_e} = -\frac{GM_e \Delta z_i}{R_e^3} \approx -0.3086 \text{ mGal/m} \tag{4}$$

where Δz_i is the difference in elevation from the reference elevation. The free air correction does not correct for the extra mass due to an increase in elevation. The Bouguer Plate correction Δg_{BP} removes the influence of this extra mass (Long and Kaufmann, 2013). The Boguer plate correction assumes the increased elevation is created by an infinite slab of thickness Δz and density p_m. The Boguer plate correction is the gravity effect due to this slab. It can be determined using the forumla

$$\Delta g_{BP} = 2\pi G \rho_B \Delta Z \approx 0.04193 \rho_m \text{ mGal/m} \tag{5}$$

Gravity surveys must also be corrected for the effect of the surrounding terrain. Both an increase or a decrease in elevation result in a decrease in the measured gravity. This is either from the upward pull of an elevation high, or the lack of mass to pull due to an elevation low. The terrain correction Δg_{terr} can be determined by computing the gravity effect due to the terrain and assuming the density of the terrain.

The Bouguer anomaly is the residual anomaly after all gravity corrections have been applied. The Boiguer anomaly isolates gravity anomalies that are due to subsurface density variations, such as the presence of an ore body. The Bouguer anomaly can be expressed at the raw gravity measurements g_{obs} with the corrections added or subtracted accordingly

$$g_B = g_{\text{obs}} - g_t + \Delta g_{\text{tide}} + \Delta g_{\text{drift}} + \Delta g_{FA} + \Delta g_{BP} + \Delta g_{\text{terr}} \tag{6}$$

If the lateral extents of a survey are much larger than the depths of an anomalous mass, the total excess mass can be calculated using the formula

$$M \approx \frac{1}{2\pi G} \iint_{z=0} g_B(x, y)\, dxdy \tag{7}$$

METHODS

Survey Methods

The gravity survey was performed over a 50 km x 50 km region centered at a latitude of 49.1286°N. The survey was conducted in 25 km x 25 km closed loops over a period of 102 days. At the end of each survey loop a final measurement was made at the same location as the first measurement of the loop. At each survey location the relative gravity measurement, the elevation and the time was recorded. An absolute gravimeter was positioned at the base station and recorded the tidal variation over time. A larger terrain survey was performed over a 150 km x 150 km grid that extented 50km to each side of the gravity survey grid. The elevation was recorded at each point in the terrain survey. The raw data was saved in column vector format and gravity corrections were made to isolate the anomaly. The corrections are described in the following sections.

Gravity Corrections

The MATLAB_2015b package was used for all data analysis.

The relative gravity measurements and tidal variation were plotted as a time series. A first-order polynomial was fit to the relative gravity measurements using the *polyfit()* function. A contour map of the topography was created using the results from the terrain survey data.

A three-column matrix **x_sort** was created using the x,y and z data. The resulting matrix was sorted first by x and then y coordinates. The unique values in **x_sort** were extracted using the *unique()* function. The sorted and unique coordinates were saved and used to extract the unique locations from the gravity data in later sections. The three columns were saved as vectors and the vectors were reshaped into matrices using the *reshape()* function. It was verified that the resulting matrices were identical to those produced by the following commands

```
Xg = 0:50,Yg = 0:50,[Xg,Yg]=meshgrid(Xg,Yg)
```

This situation was due to the regular spacing of the survey points. For irregularly spaced data, some form of interpolation might be needed in order to create contour plots from the data.

A new vector **g_corr** was initialized using the relative gravity measurements and was updated for all of the gravity corrections. A contour plot of the raw absolute measurements was created.

The IGF (Eqn 1) was used to compute the value of theoretical gravity at the centre of the grid. The gravity data was updated by subtracting this value. A contour plot of the data after lattitude corrections was created.

The tidal correction was applied by subtracting the relative tidal measurements made at the base station from the gravity data. A contour plot of the data after tidal correction was created. The drift correction was determined by computing the drift correction over each individual survey loop. The drift correction at each point in the survey loop was determined

using equation 2. The total drift over the loop was then subtracted from all of the future data points. The overnight drift was then corrected by subtracting the value at the first station on the next loop from all future data points. This process was repeated over the entire dataset.

A time series plot of the data after drift correction was plotted and compared to the raw time series plot. The data was reshaped into a grid for the remaining corrections.

The mean elevation over the terrain survey was chosen as the reference elevation for elevation corrections. The free-air correction was applied at each survey point using equation 4. The value for Δz_i was determined by subtracting the reference elevation from the survey elevation. A contour plot of the data after free-air correction was created. The Bouguer plate correction was applied at each survey point using equation 5 assuming that the surface had an average density of $2.65\,\mathrm{g/cm^3}$. The value for Δz_i was the same as was used for the free air correction. A contour plot of the data after the Bouguer plate correction was created.

The terrain correction was applied by computing the gravity effect at each survey point due to the surrounding terrain. The average density of the terrain was assumed to be $2.65\,\mathrm{g/cm^3}$. A function *grav_eff_point()* function was created to compute the gravity effect at a point $\mathbf{x_i}$, due to a mass m at point $\mathbf{x_m}$. For each survey point, a position vector $\mathbf{x_1}$ was created with its x and y coordinates and a z coordinate equal to the reference elevation. The terrain correction at the survey point was computed by summing up the gravity effect due to each point on the terrain survey. At each terrain point, a position vector $\mathbf{x_m}$ was created using its x and y coordinates and a z-coordinate equal to half of the distance between its elevation and the reference elevation. The mass of this terrain block dm was computed by multiplying the density by the volume of the block, which was equal to the grid spacing times the difference from the block elevation to the reference elevation. The resulting position vectors and mass were input into *grav_eff_point* and the absolute value of its output was added to the terrain correction at the current survey point (because the terrain correction is always positive). This procedure was repeated for each terrain point to obtain the overall terrain correction at the survey point. This was repeated at every survey point on grid. The computation was achieved using a double nested loop. The code for the loop is shown below.

```
dg_terr = zeros(size(g_corr,1)); %initialize a terrain correction
    array
%loops through each survey point
for i = 1:size(dg_terr,1)
    for j = 1:size(dg_terr,2)
        xi = [Xg(i,j)*1000,Yg(i,j)*1000,z_datum];
        %loops through all points in the terrain data
        for ii = 1:size(Xt,1)
            for jj = 1:size(Xt,2)
                xm = [Xt(ii,jj)*1000,Yt(ii,jj)*1000,0.5*(Zt(ii,jj
                    )-z_datum)];
                dm = rho_B*1000*(Zt(ii,jj)-z_datum)*dA;
                g_eff = abs(grav_eff_point(xi,xm,dm,G));
                dg_terr(i,j) = dg_terr(i,j) + g_eff; %increment
                    the current value of dg_terr
```

```
            end
        end
    end
end
```

The resulting terrain correction was added to the corrected gravity data, and the result was the Bouguer anomaly. The regional anomaly was subtracted from the Bouguer anomaly to obtain the anomaly due to the buried ore deposits.

Extent and Mass of Anomaly

The lateral extent of the anomaly was further investigated by plotting the horizontal derivative of the gravity data. Equation 7 was used to determine the excess mass of the anomaly. The gravity data was integrated over the region from 5 km to 23 km in the E-W direction and from 23 km to 40 km in the S-N direction. The integration was performed by multiplying the value of the gravity anomaly at each grid point, multiplying it by the area element dA and summing over the entire region. The code for the integration is shown below.

```
contourf(Xg,Yg,dgzz); %plot data
xlabel('Easting [km]','FontSize',ax_font);
ylabel('Northing [km]','FontSize',ax_font);
axis('equal');
h_c = colorbar();
xlabel(h_c,'Gravity $\mu$Gal','Interpreter','latex','FontSize',
    ax_font);
print('-dpdf','-r220',['dgzz.pdf']) %savefile
```

RESULTS

The raw gravity measurements and the tidal variation recorded at the base station is shown in figure 1. The gravity measurements appeared to be correlated to the tidal variation. The gravity measurements showed a periodic trend in the local high and low measurements with an amplitude on the order of 100 mGal and period on the order of 1000 h. These periodic high and lows appeared to be of the same magnitude, frequency and phase of the tidal variation. This suggests that the tidal variation had a significant effect on the recorded data. The data also showed a general upward trend in the gravity measurements. The best fit line in figure 1 highlights this observed trend. This trend did not appear to be related to a spatial variation over the survey area, but instead to a time-related variation such as instrument drift.

The topography of the survey area and its immediate surroundings is shown in figure 2. The region had relatively small elevation changes over large horizontal distances. The elevation range was 10.9626 m, with a mean elevation of 3000.0134 m. The region showed three prominent elevation lows of magnitude 2994.5334 m and three elevation highs of magnitude 30 005.496 m. The overall topographic shape seemed similar to a stretched 2-dimensional sinusoid. The survey grid was located directly between one of the elevation high and low points.

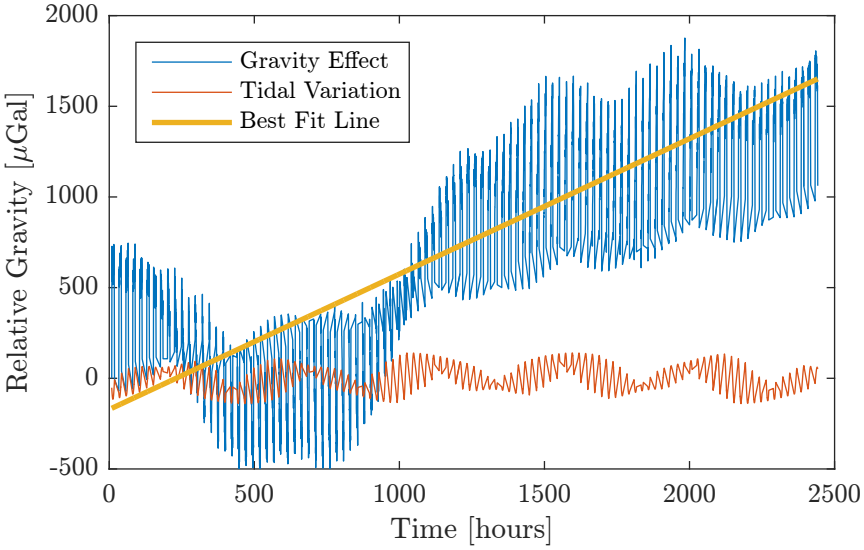

Figure 1: Time variation of relative gravity measurements and the tidal variation. A best fit of the relative gravity measurements is shown to highlight the overall trend of its time variation. An overall upward trend of the gravity measurements can be seen. A correlation between the tidal effect and measured gravity can also be seen.

The raw absolute gravity data is shown in figure 3. There was a prominent gravity low with a magnitude of 9.809 918 m/s^2 in the western area of the survey grid. At about 25 km on the E-W axis of the grid there was a region with a very clear and sharp increase in the gravity measurements. This increase was attributed to instrument drift and the survey design and will be discussed in later paragraphs. The gravity measurements appeared to increase from east to west, and were somewhat symmetrical from south to north.

The theoretical gravity at the centre of the grid was determined to be 980 992 497.8439 µGal. This value was subtracted from all points on the grid. This method may have led to a significant source of error in the results because the normal gravity was assumed to be constant over the survey grid. However, moving north along the survey area would change the theoretical gravity by an appreciable amount. A better technique would be to compute the theoretical gravity at each point and apply the individual corrections to the data. Figure 4 shows the data after the latitude correction had been applied. The shape of the plot was unchanged and simply had a constant value subtracted from all points. After the latitude correction there was a residual value of −260.1794 µGal. This residual value was likely due to local effects, such as terrain and elevation, as well as large scale regional effects that caused a difference in gravity from that predicted by the IGF. Some of the difference in the residual value may also have been due to the target anomaly.

Figure 5 shows the data after the tidal correction had been applied. There were subtle differences in the shape of the plot. The region with higher gravity in the eastern area of the grid had a slightly greater magnitude, and was shifted to the north. The tidal correction accounted for the relative position of the sun and moon, which have the greatest tidal influence on gravity measurements.

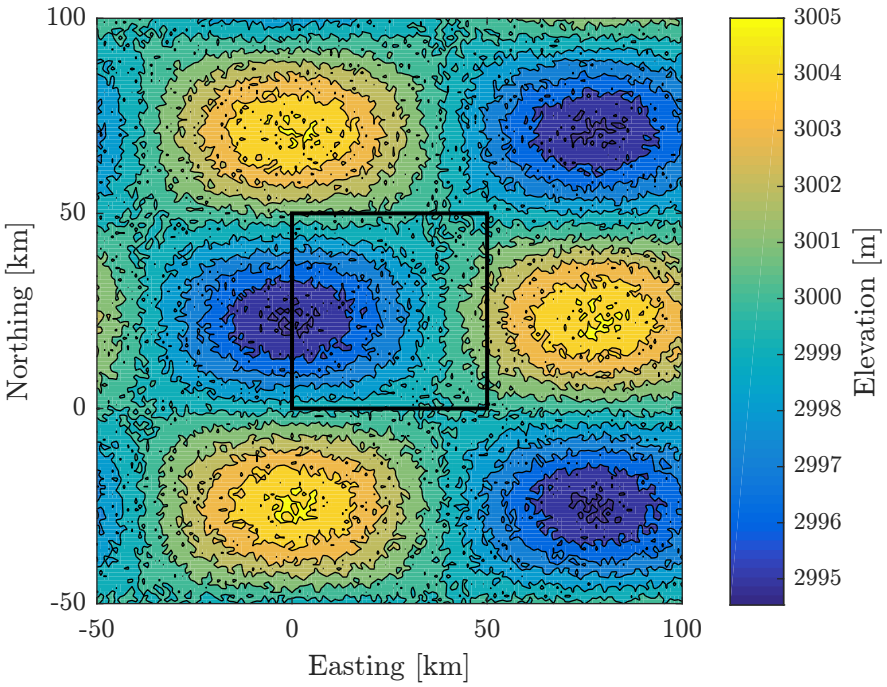

Figure 2: Contour map showing elevation in the gravity survey region and the surrounding region (±50km). There was a topographic peak with elevation of 3005m at the east end of the survey area, and a valley with elevation of 2995m at its west end. The total elevation variation over the greater survey region was approximately 10m. The location of the survey grid is outlined in black.

A plot of the gravity measurement time series after the tidal and drift correction is shown in figure 6. There were two major differences between the corrected and raw time series (fig 1). The first difference was that the number of local maxima/minima was decreased in the corrected time series. This difference was likely due to the tidal correction. In the corrected time series, there were only one local minima and two local maxima with wavelengths greater than one day. The other difference was the data did not show the linear increase that was visible in the raw time series. This was likely due to the drift correction.

Figure 7 shows the gravity data after the drift correction. The sharp increase along the 25 km easting coordinate was no longer visible. This suggests that the the rapid increase in the raw data was due to a time varying process such as instrument drift. This result made sense, because the survey was done in loops starting in the western half and ending in the eastern half of the survey area. Therefore the gravity readings in the eastern half of the grid would have been higher than in the western half due to the increase in readings over time. The data was also much more symmetrical in the N-S direction. The overall shape still showed a gravity low in the west and a gravity high in the east area of the grid. The data appeared to be correlated with the topography of the region (fig 2).

Figure 8 shows the gravity data after the free air correction. The gravity low in the western region became a gravity high, and the gravity high in the western region became a gravity low. The overall range of gravity values decreased. These results made sense because the

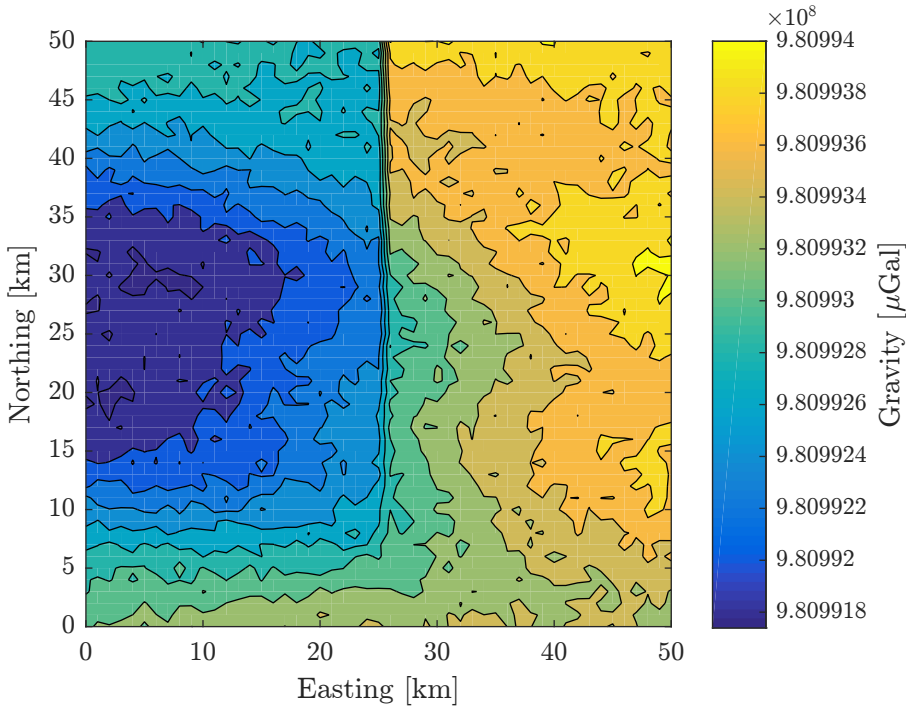

Figure 3: Contour plot of raw gravity measurements. There was a gravity low with a magnitude of 9.909918 m/s^2 in the central western area of the survey grid and a gravity high with a magnitude of 9.80994 m/s^2 in the central eastern area of the survey grid. There was a very large change in gravity measurements over a short distance along the line x=25 km.

gravity low was in a region of low elevation. The free air correction would be positive in the areas below the reference elevation and negative in areas above the reference elevation because Δz_i in equation 4 would be negative and positive respectively.

Figure 9 shows the gravity data after the Bouguer plate correction. The data was more similar to how it appeared before the terrain correction with a gravity low in the western region and a gravity high in the eastern region. This was expected because the Bouguer plate correction should decrease the corrected data in regions below the reference elevation and increase the corrected data in regions above the reference elevation. The data after the elevation correction very closely approximated the shape of the terrain. The range of the corrected gravity measurements was decreased to about 450 µGal.

Figure 10 shows the gravity data after the Terrain correction. What was left was the Bouguer anomaly. The target ore body was clearly visible in the northwest region of the survey area. The ore body produced an irregularly shaped negative gravity anomaly. There was still a large regional anomaly with a mean value of 502.7422 µGal.

Figure 11) shows the Bouguer anomaly with the regional anomaly removed. The data appeared exactly the same as in figure 10 except with a shifted range of gravity measurements. The negative gravity anomaly extended from 5 km to 23 km in the E-W direction and from 23 km to 40 km in the S-N direction. The anomaly appeared to be composed of three regions

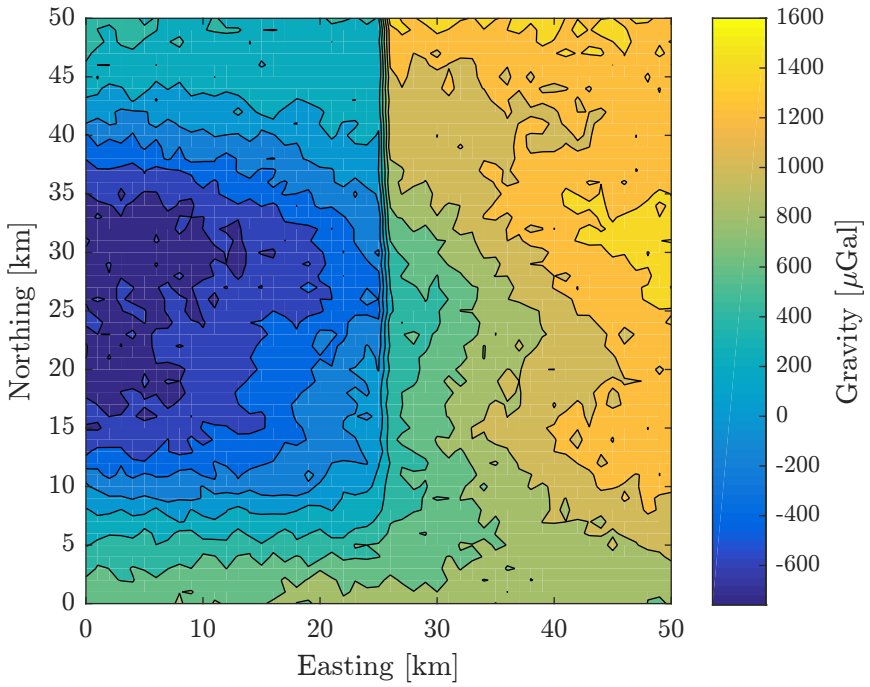

Figure 4: Contour plot of gravity measurements after normal gravity correction has been applied. The data are similar to the raw measurements but with the theoretical gravity at the centre of the survey grid (determined by the IGF) subtracted from them.

with negative gravity anomalies. There were two large gravity anomalies centred over the coordinates (10,29) and (18,30) with a minimum value of $-3.6836\,\mu$Gal. There was also a smaller gravity anomaly centered over (13,37). The highest concentrations of anomalous mass appeared to be centred over these gravity lows. The horizontal derivative is shown in figure 12. The lateral extent, and individual sections of the ore body were more clearly visible using the derivative technique.

The ore body was centred at a depth of approximately 1000 m, which was considerably more shallow than the extent of the survey grid. Therefore, equation 7 held as a good estimate of the anomalous mass. The region highlighted in figure 11 was used as the integration boundary. The total mass of the ore body was estimated to be 5.3×10^9kg.

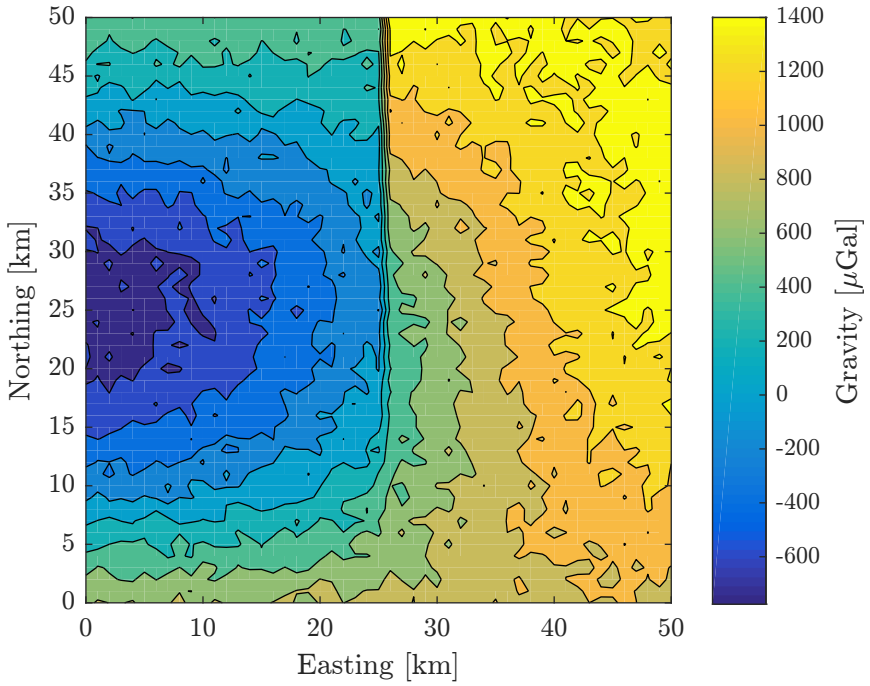

Figure 5: Contour plot of gravity measurements after tidal correction has been applied. There was still a gravity low in the central western area of the survey grid. The gravity high in data is more to the northwest in the tidally corrected data than in the raw data.

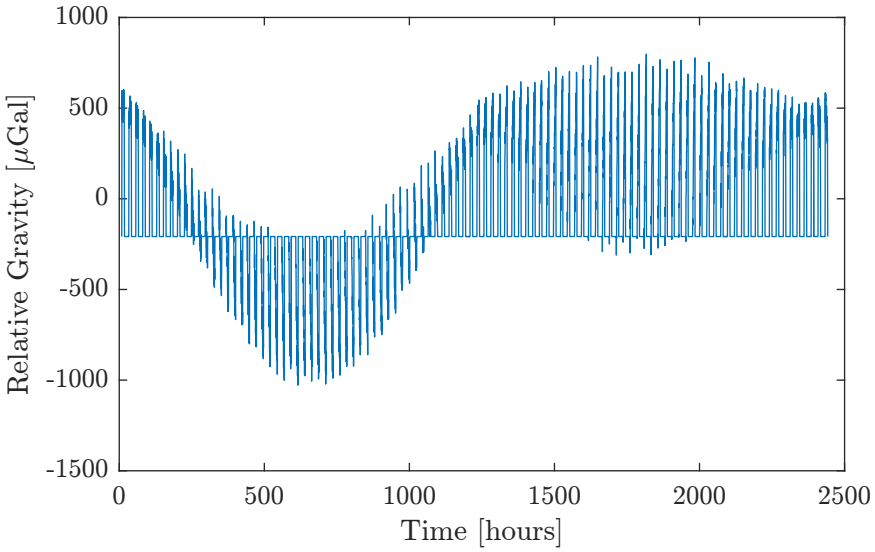

Figure 6: Time series of gravity data after tidal and instrument drift corrections applied. The data no longer showed a linear increase over time, and the medium-wavelength variations due to tidal effects were removed.

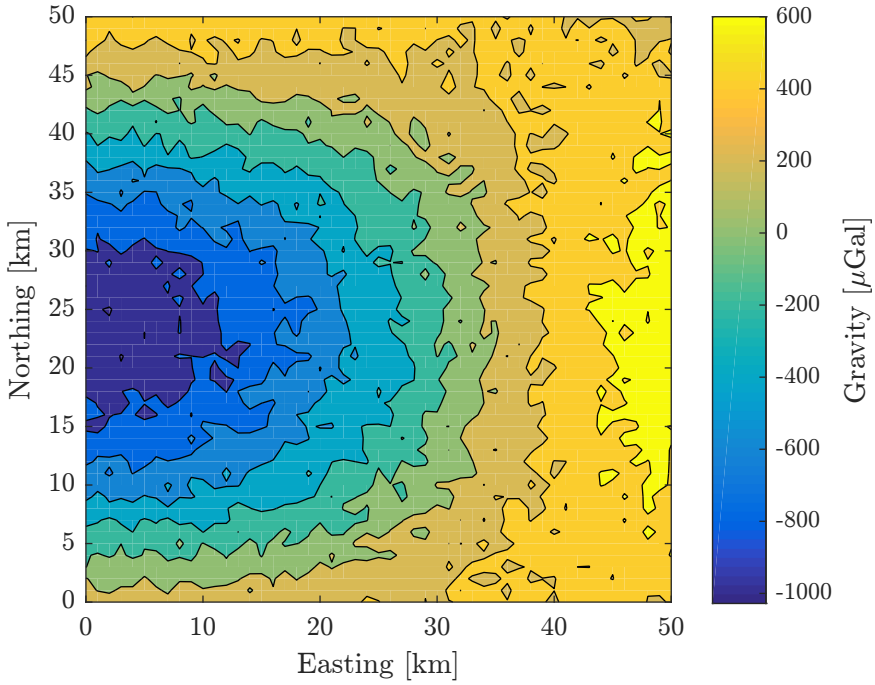

Figure 7: Gravity measurements after instrument drift correction applied. The sharp increase in gravity along the line x=25 km was no longer visible after the correction. The data appeared to be more symmetrical along the line y =25 km, and resembled the profile of the grid topography.

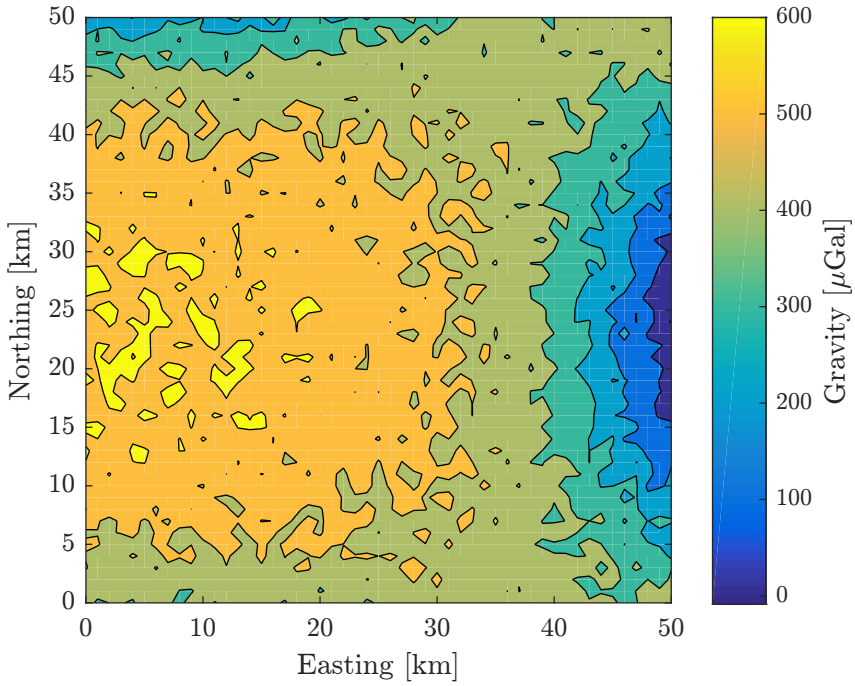

Figure 8: Gravity measurements after free air correction. The gravity low in the western region was replaced by a gravity high and the gravity high in the eastern region was replaced by a gravity low.

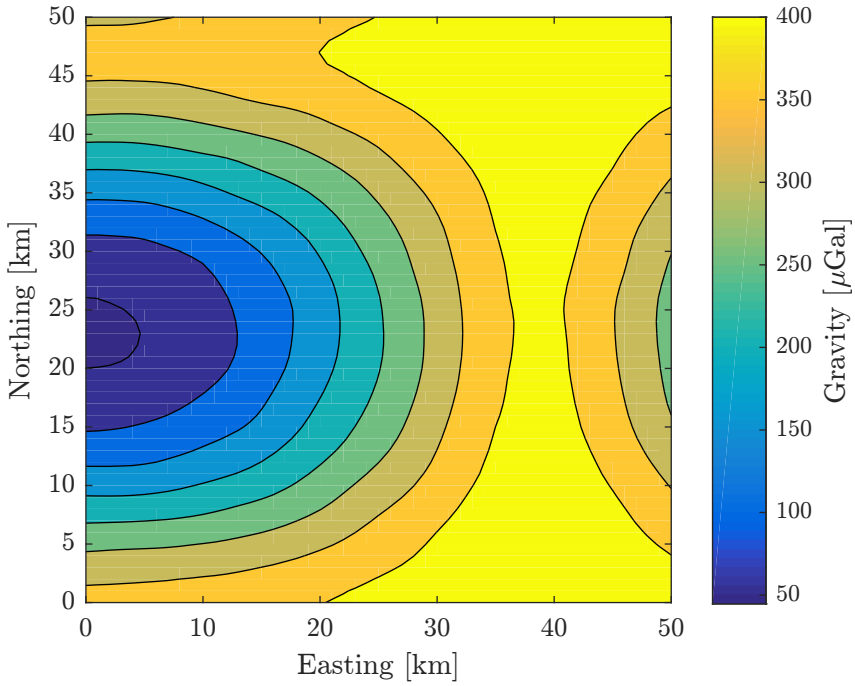

Figure 9: After elevation correction. The data appeared very regular and closely approximated the terrain.

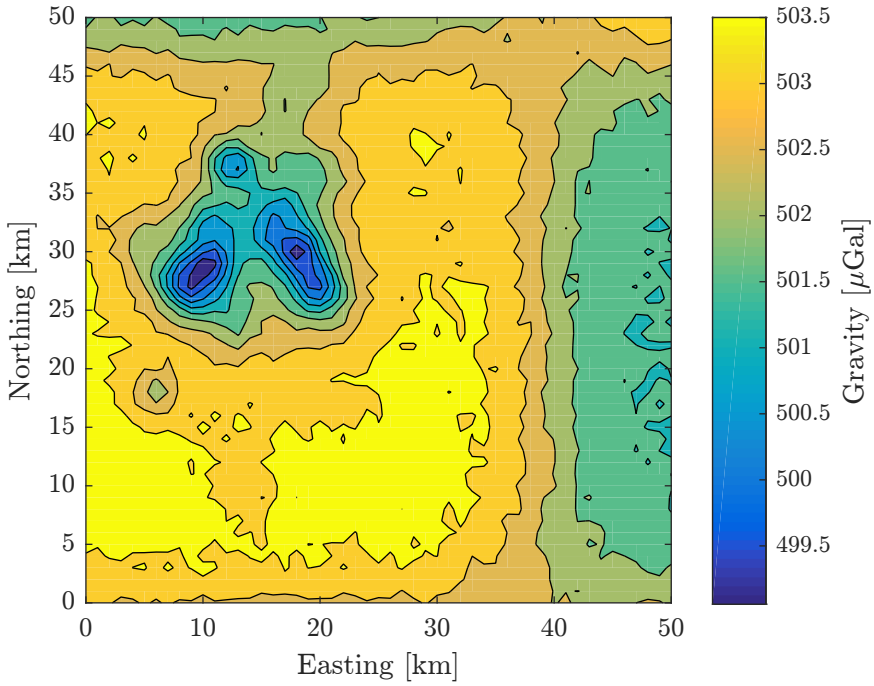

Figure 10: Bouguer anomaly after all gravity corrections were applied. The gravity effect of the ore deposit was clearly visible. There appeared to be a large-large scale regional anomaly with average magnitude of 502.7422 µGal.

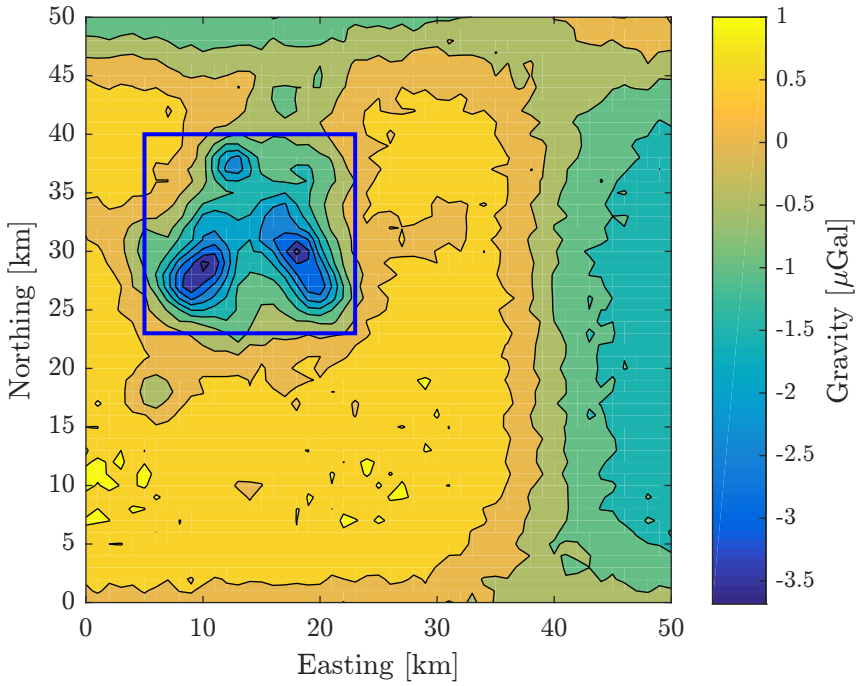

Figure 11: Bouguer anomaly with regional correction applied. The approximate borders of the anomaly (and the grid for the excess mass calculation) is outlined in blue.

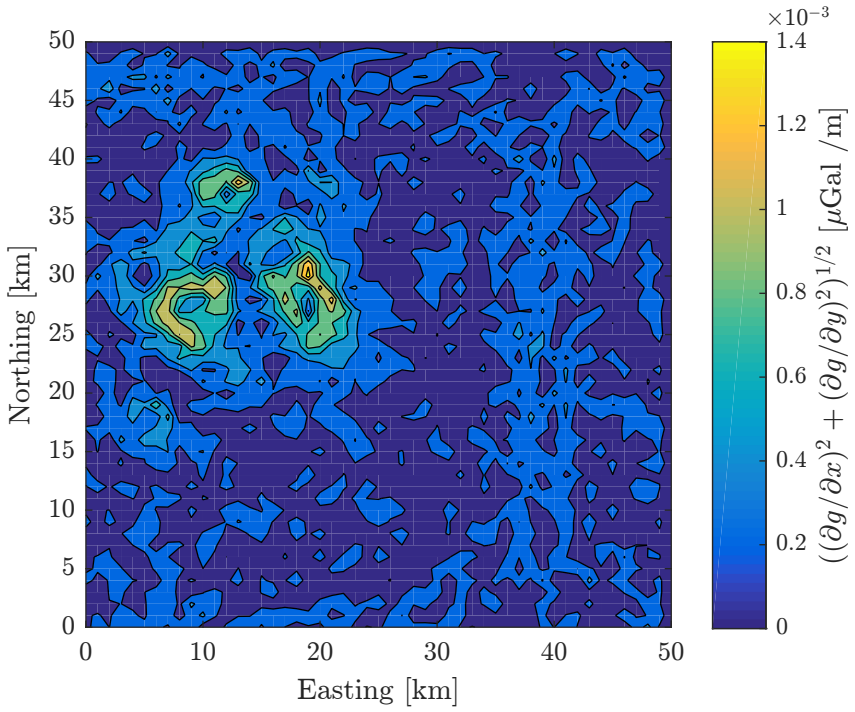

Figure 12: Horizontal Derivative of gravity data. The ore deposit appeared to contain three smaller desposits.

CONCLUSION

An ore deposit with an estimated mass of 5.3×10^9kg was identified using a gravity survey. The magnitude of the gravity anomaly was 3.6836 µGal. This magnitude was much smaller than the raw gravity measurements and therefore latitude, tidal, instrument drift, elevation and terrain corrections were required to see the gravitational effects of the anomaly. After the corrections were made, the extent of the anomaly was clearly visible. This exercise demonstrated the importance of proper gravity corrections on gravity data in order to make inferences about subsurface density variations.

REFERENCES

H. Burger, A. Sheehan, and C. Jones. *Introduction to Applied Geophysics: Exploring the Shallow Subsurface*. W.W. Norton and Company, 2006. ISBN 0-393-92637-0.

B. Karwchewski. *GOPH 547 - Gravity and Magnetics Lab Assignment #2*. University of Calgary, 2016.

Leland Long and Ronald Kaufmann. *Acquisition of Terrestrial Gravity Data*. Cambridge University Press, 2013. ISBN 978-1-107-02413-7.

H. Moritz. Geodetic reference system 1980. *Journal of Geodesy*, 74(1): 128–133, 2000. ISSN 1432-1394. doi: 10.1007/s001900050278. URL `http://dx.doi.org/10.1007/s001900050278`.